Multistage Unfolding of Wheat Germ Ribosomal 5S RNA Analyzed by Differential Scanning Calorimetry†

Shi-Jiang Li and Alan G. Marshall*,‡

Department of Biochemistry, The Ohio State University, Columbus, Ohio 43210

Received November 7, 1984

ABSTRACT: Unfolding of purified wheat germ ribosomal RNA has been studied by differential scanning calorimetry (DSC) from 15 to 95 °C, in the presence and absence of 100 mM NaCl and/or 10 mM $MgCl_2$. The total enthalpy of melting varies from about 290 (no sodium or magnesium) to 480 kcal/mol (Mg^{2+} only) and precisely accounts for the number and types of base pairs deduced from prior Fourier-transform infrared experiments. The composite DSC curves are analyzed into four individual two-state melting stages. Both Na^+ and Mg^{2+} shift the melting transitions to higher temperature; in addition, Mg^{2+} causes the individual transitions to merge (i.e., melt cooperatively) and leads to irreversible chain cleavage at high temperature. The results are analyzed according to three general secondary base-pairing models for eukaryotic 5S RNA.

Although the primary sequences of more than 100 ribosomal 5S RNAs are known (Erdmann et al., 1984), and one 5S RNA has been crystallized (Morikawa et al., 1982), there is as yet no X-ray diffraction structure of any 5S RNA. It is widely speculated that all eubacterial 5S RNAs share a common secondary base-pairing structure (Singhal & Shaw, 1983), and several general secondary base-pairing schemes have been proposed (Fox & Woese, 1975; Nishikawa & Takemura, 1978; Luoma & Marshall, 1978a,b; Studnicka et al., 1981).

Several techniques previously tested on transfer RNAs (tRNAs) have now been applied to 5S RNA: ultraviolet hyperchromism, circular dichroism, and Fourier-transform infrared spectrometry (Burkey et al., 1983; Chang et al., 1984a; Li et al., 1984a); Raman spectrometry (Luoma & Marshall, 1978a,b): electron spin resonance spin-label spectrometry (Luoma et al., 1982); ^1H (Luoma et al., 1980; Burns et al., 1980; Salemink et al., 1981; Kime & Moore, 1983a,b), ^{19}F (Marshall & Smith, 1980), and ^{31}P (Salemink et al., 1981) nuclear magnetic resonance spectrometry. Although differential scanning calorimetry (DSC) studies on tRNAs (Privalov et al., 1975; Privalov & Filimonov, 1978; Schott et al., 1981) and one prokaryotic 5S RNA (Matveev et al., 1982) have been reported, no DSC studies of eukaryotic ribosomal 5S RNA have yet been published. "Differential thermal melting" [e.g., see Ohta et al. (1983)] is based on the slope of a UV-melting curve and should not be confused with a true DSC experiment.

In this paper, we report a DSC analysis of thermal melting for a eukaryotic (wheat germ) 5S RNA, based on newly available on-line computer analysis of digitized DSC data (Chang et al., 1984b). Experiments were conducted in the presence and absence of Na^+ and/or Mg^{2+}, to investigate the structure-stabilizing effects of these two important cations. Unlike the other physical techniques, whose temperature dependence reflects only those changes which affect the "reporter groups" involved, the DSC measurement detects *all* structural features whose removal requires energy (e.g., base-pair hydrogen bonds, base stacking, metal ion mediated intrachain phosphate links, etc.) and thus provides a direct measure of thermodynamic stability for comparison to proposed secondary structural models or segments.

Materials and Methods

Wheat germ was obtained as a gift from International Multifoods, Columbus, OH 43208. Wheat germ 5S RNA was isolated by phenol/sodium dodecyl sulfate (SDS)[1] extraction, followed by ion-exchange and gel filtration chromatography as described previously (Li et al., 1984b). The 5S RNA samples in 10 mM sodium cacodylate buffer (pH 7.0) were prepared under four different salt conditions: (A) no Na^+ or Mg^{2+}; (B) 100 mM NaCl; (C) 10 mM $MgCl_2$; (D) 100 mM NaCl and 10 mM $MgCl_2$. Approximately 30 mg of 5S RNA was divided into four aliquots, each placed in small dialysis tubing (1 mL volume, Spectrapor membrane tubing 2, molecular weight cutoff = 12 000–14 000). Samples with Mg^{2+} were dialyzed against their respective buffers. Samples without Mg^{2+} were prepared by dialysis first against buffer containing 10 mM Na_2EDTA and then against buffer A or B. All dialyses were repeated 4 times at a volume ratio of 1000:1 for 6 h, stirring at 4 °C. Each final dialysis buffer was used as the reference sample for calorimetry measurements. The 5S RNA DSC samples were 98% pure according to slab gel electrophoresis (Li et al., 1984b).

RNA concentrations were determined according to Burkey et al. (1983). The molar concentration in each digest was calculated from published extinction coefficients at 260 nm for the 5′-phosphates in alkaline solution, expressed as moles of phosphate (Dawson et al., 1969). Wheat germ 5S RNA concentration (from moles of phosphate residues after alkaline hydrolysis) was based on an extinction coefficient of 10 450 M^{-1} cm^{-1} computed from the published extinction coefficients for the component 5′-monophosphates and the known RNA primary sequence (Barber & Nichols, 1978; MacKay et al., 1980). The four sample concentrations were (A) 1.59×10^{-4}, (B) 1.72×10^{-4}, (C) 1.14×10^{-4}, and (D) 1.67×10^{-4} M.

DSC data acquisition and analysis were as described by Chang et al. (1984b). In order that each scan begin at 15 °C, it is necessary to bring the whole system first to 0 °C. Room temperature was set at 12 °C to minimize moisture conden-

† This work was supported by grants (to A.G.M.) from the U.S. Public Health Service (NIH 1R01 GM-29274) and The Ohio State University.

‡ A.G.M. is also a member of the Department of Chemistry.

[1] Abbreviations: SDS, sodium dodecyl sulfate; EDTA, ethylenediaminetetraacetic acid.

0006-2960/85/0424-4047$01.50/0

Table I: Thermodynamic Parameters for Multistage Melting of Wheat Germ 5S RNA[a]

sample	Na^+ (M)	Mg^{2+} (mM)	peak	T_m - 273.2	ΔH (kcal/mol)	$\Delta H_{sim}/\Delta H_{exp}$ = ratio	ΔG^{298} (kcal/mol)[b]	total ΔG^{298} (kcal/mol)
A	none	none	1	26.5	60.5	289.4/284.9 = 1.02	0.30	10.38
			2	34.7	78.2		2.47	
			3	39.5	72.6		3.37	
			4	42.1	78.1		4.24	
B	0.1	none	1	43.1	65.7	366/371 = 0.99	3.76	31.48
			2	50.2	103.1		8.04	
			3	55.3	101.2		9.34	
			4	61.6	94.5		10.34	
C	none	10	1	52.3	58.0	481.9/478.0 = 1.01	4.87	60.95
			2	64.3	99.3		11.57	
			3	70.3	238.8		31.51	
			4	78.2	85.8		13.00	
D	0.1	10	1	59.3	58.4	389.8/398.3 = 0.98	6.03	51.09
			2	65.8	96.5		11.62	
			3	72.1	130.8		17.85	
			4	77.5	104.1		15.59	

[a] ΔH_{exp} is the enthalpy of melting obtained directly from the total area under the composite DSC peak. ΔH_{sim} is the total enthalpy of melting obtained by adding up the enthalpies (ΔH) for each of the simulated component DSC peaks. T_m for each simulated DSC component is the melting midpoint for that two-state transition. Also listed are the component (ΔG^{298}) and total (total ΔG^{298}) free energies of melting. [b] $\Delta G^{298} = \Delta H(T_m - 298)/T_m$.

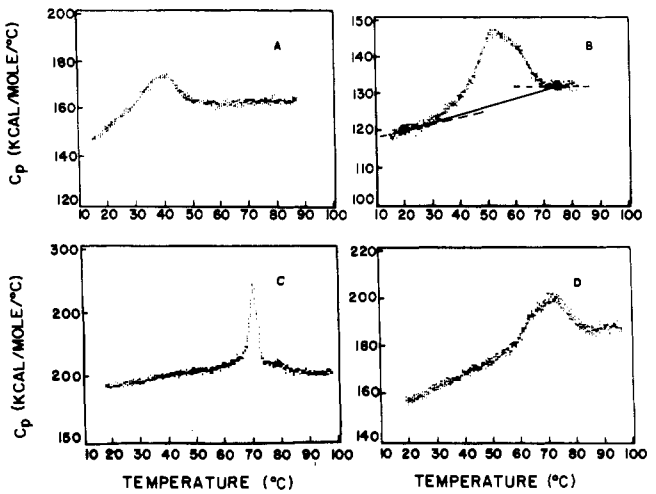

FIGURE 1: Differential scanning calorimetry plots for wheat germ 5S RNA, in 10 mM sodium cacodylate buffer, pH 7.0, for four different salt conditions: (A) no added NaCl or $MgCl_2$; (B) 100 mM NaCl (see text for treatment of base line); (C) 10 mM $MgCl_2$; (D) 100 mM NaCl and 10 mM $MgCl_2$. The calorimeter output has been conditioned and digitized. The y offset is arbitrary. Scan rates varied from 70.1 to 72.8 K/h. The data have not been filtered or smoothed in any way.

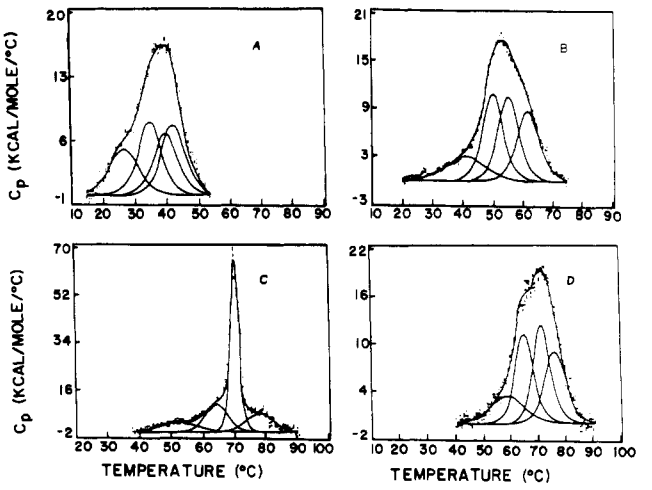

FIGURE 2: Data of Figure 1 are replotted after a seven-point smoothing and linear base-line correction over the transition region. Panels A–D are as in Figure 1. In each plot, the thin lines represent the minimum number of two-state component transitions required to fit the experimental curve. The composite dark line is the sum of the component transition peaks.

sation during the precool step. Sample and reference volumes were each 0.7 mL.

RESULTS

Wheat germ 5S RNA melting profiles for four different salt conditions are shown in Figure 1. These curves represent raw data (i.e., unsmoothed, with no base-line correction). Minor variation in the y offset from scan to scan is due to differences in base-line offset voltage and does not affect the peak profile. A common feature of all four curves is a decrease in base-line slope passing through the melting transition, as has been commonly observed and described in earlier work (Privalov, 1974; Krishnan & Brandts, 1978). The heat capacity of the unmelted form increases with temperature, but the heat capacity of the melted form is independent of temperature. Thus, for each two-state melting process, the base-line slope will change according to the fraction melted, ϕ, as a function of temperature. The simplest approximation (and, for multiple unresolved transitions, the only practical choice) is a base line drawn from the leftmost to rightmost DSC ordinates at which the data begins to deviate detectably from straight-line fits to the low- and high-temperature slopes (see Figure 1B).

The four DSC data sets of Figure 1, after a seven-point smoothing and base-line tilting, are replotted in Figure 2. CURFIT analysis of the reduced data according to a two-state melting model for each component transition gives the overlapping individual peaks shown in Figure 2, and their sum is shown as a solid line for comparison to each experimental DSC curve.

The melting midpoint (T_m) and enthalpy of melting (ΔH) for each simulated component peak are listed in Table I, for each of the four salt conditions. Provided that the temperature range for simulation was wide enough to include the full DSC composite peak envelope, T_m and ΔH for the simulated component peaks were not especially sensitive to the low- and high-temperature cutoffs (see Figure 1B) used to define the DSC peak. The low-temperature cutoff defines the native state of 5S RNA in solution, and the high-temperature cutoff defines the fully denatured state; beyond either limit, the base line is nearly straight. Attempts (not shown) to simulate with fewer than four component transitions gave poor fits; using more than five components gave no significant improvement.

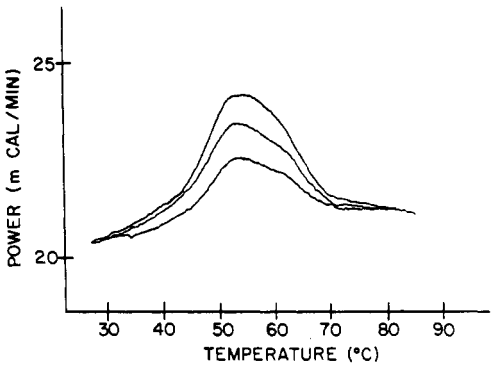

FIGURE 3: DSC power vs. scan temperature, for three scan rates: 96.5 K/h (top), 67.4 K/h (middle), and 48.9 K/h (bottom). Although the signal strength increases with scan rate, the curve shape remains the same (see Table II). Thus, the present results are independent of scan rate.

Table II: Effect of DSC Scan Rate upon T_m for Component Melting Transitions of Wheat Germ 5S RNA in the Presence of 0.1 M NaCl with No Added $MgCl_2$[a]

DSC scan rate (K/h)	melting midpoint, T_m − 273.2 (K)			
	peak 1	peak 2	peak 3	peak 4
48.9	41.6	50.0	55.3	61.7
67.4	43.1	50.2	55.3	61.6
96.4	41.1	50.1	55.1	61.7

[a] Peaks are numbered as in Table I.

Effect of Scan Rate. Figure 3 presents plots of DSC power vs. temperature for three different scanning rates. (The scanning rate was calculated after the data were acquired.) Faster scanning produces larger peaks and thus better signal-to-noise ratio. However, scanning too fast might distort the DSC curve, due either to insufficient transient response from the calorimeter itself or to insufficient time for equilibrium to be established at each temperature as the temperature changes during the scan. The best-fit analyses of the results for each scan rate are compared in Table II. The close agreement between the results from different scan rates indicates that the scan rates are sufficiently slow to yield reliable data.

Reproducibility and Reversibility. DSC scans for two separate aliquots from the same 5S RNA solution are analyzed in the top and bottom rows of Table III. The excellent reproducibility of the results is seen from the good agreement (to within 1.5% in all but one value) between the T_m and ΔH values for the two scans. Reversibility of the experiment was tested as follows. After aliquot A was scanned from low to high temperature, it was allowed to recool at 0.2 K/min (i.e., 5 times slower than the DSC scan rate) and then scanned again. Comparison of the top and middle rows of Table III shows that the scan is indeed reversible, except for a 10% reduction in T_m and ΔH for the lowest temperature transition for the rescan, as seen in Figure 4. Similar results were seen for 5S RNA with no added salt.

Quite different results were observed for samples containing 10 mM $MgCl_2$ (with or without 0.1 M NaCl). In these cases,

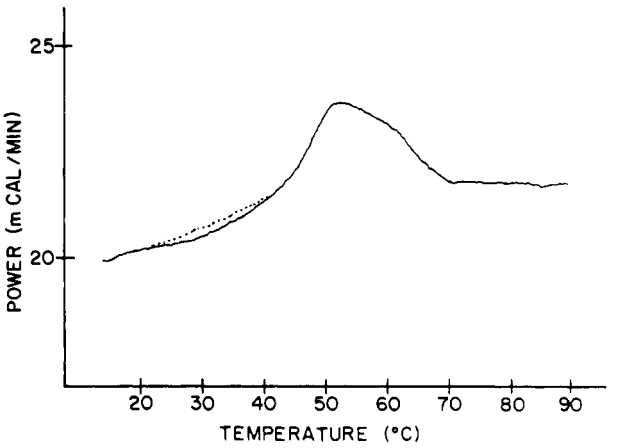

FIGURE 4: Reversibility of DSC experiment for wheat germ 5S RNA in the presence of 0.1 M NaCl and no added Mg^{2+}. (—) First scan at 67.4 K/h; (– – –) second scan at 67.2 K/h. Except for the initial melting region ($T < 40$ °C), the curves superimpose, indicating a reversible unfolding process.

a rescan (not shown) gave a nearly flat base line, indicating that the 5S RNA is irreversibly degraded after exposure to Mg^{2+} at high temperature (90 °C). Slab gel electrophoresis (not shown) performed on Mg^{2+}-containing 5S RNA samples before and after a DSC scan confirmed that the RNA polyribonucleotide chain had been broken in several places.

Discussion

Suppose that a macromolecule consists of n domains, each with different thermodynamic enthalpy of melting, and that those domains melt independently. Further denote a given conformation according to whether a given domain is melted (0) or unmelted (1). Next, rank the domains in order of decreasing free energy of melting, with the most stable domain listed first. For example, a four-domain system for which the two most stable domains are unmelted and the remaining two are melted might be described as (1,1,0,0), representing one of the $2^n = 16$ possible free energy states.

When such a system melts reversibly, all 2^n states are in mutual equilibrium, and the system is expected to progress sequentially from lowest to highest energy states (Freire & Biltonin, 1978):

$$(1,1,1,1) \rightarrow (1,1,1,0) \rightarrow (1,1,0,1) \rightarrow (1,0,1,1) \rightarrow \ldots \rightarrow (0,0,0,0) \quad (1)$$

For example, in the $(1,1,1,0) \rightarrow (1,1,0,1)$ step, the macromolecule has to break a more stable domain and simultaneously re-form a less stable domain. Fortunately, when the domains differ significantly in stability, only $n + 1 = 5$ states are significantly populated (Matveev et al., 1982), and the melting process simplifies to

$$(1,1,1,1) \rightarrow (1,1,1,0) \rightarrow (1,1,0,0) \rightarrow (1,0,0,0) \rightarrow (0,0,0,0) \quad (2)$$

If the domains do not differ signicantly in stability (e.g., T_m values differ by <3K or so), then the more general mechanism applies. However, in such cases the DSC peaks overlap so closely that they cannot be distinguished reliably (Freire &

Table III: Reproducibility and Reversibility of DSC Scans for Wheat Germ 5S RNA in the Presence of 0.1 M NaCl with No Added $MgCl_2$[a]

			T_m − 273.2 (K)				ΔH (kcal/mol)			
		scan rate (K/h)	1	2	3	4	1	2	3	4
aliquot A	scan	67.4	43.1	50.2	55.3	61.6	65.7	103.1	101.2	96.5
	rescan[b]	67.2	40.8	50.0	55.2	61.8	59.9	100.9	103.1	93.4
aliquot B	scan	67.5	43.0	50.4	55.3	61.7	58.3	104.5	99.7	94.4

[a] Peaks are numbered as in Tables I and II. Two aliquots were taken from the same 5S RNA solution. [b] The same sample was cooled slowly and another DSC scan taken.

Biltonen, 1978). In other words, reliable data reduction is possible only when T_m values for successive transitions differ by ≥5K, so that mechanism 2 applies, and one should not attempt to resolve additional states. It remains only to decide how best to analyze the DSC scan for such a system into its n component peaks.

Filimonov et al. (1982) have proposed that the analysis begin by fitting the highest temperature transition by using the highest temperature portion of that peak. They argue that overlap with other peaks is minimal at the highest temperature end of the scan and that the first transition can thus be fitted most accurately. Assuming that the first transition fit is correct, they then proceed to the next highest temperature transition, and so on in sequence. In this paper, we use the method of Chang et al. (1984b), in which all of the transitions are fitted simultaneously using a CURFIT algorithm. The sequential-fitting method propagates errors which accumulate in proceeding from highest to lowest temperature transitions, whereas the CURFIT approach uses the full DSC curve to judge the quality of the fit, so that errors are equally distributed among all of the peaks.

The excellent agreement (±2%) between the total enthalpy of melting (ΔH_{exp}) obtained as the area under the experimental DSC envelope and the total enthalpy of melting (ΔH_{sim}) computed from the sum of the ΔH values for the simulated component transitions in each case (see Table I) strongly supports the validity of a two-state model for each transition and the choice of a linear base-line approximation (Jackson & Brandts, 1970; Privalov, 1974). In addition, the two-state model based on the true thermodynamic DSC peak shape is superior to previous Gaussian fits which lack any theoretical relevance (Privalov et al., 1975). For example, the height and width of a Gaussian peak are independently adjustable, whereas the height and width of a true DSC two-state transition are not independent (Chang et al., 1984b).

For each of the four salt conditions, the DSC base-line slope is positive and linear at temperatures below the RNA transitions and nearly zero at temperatures above the transitions. The heat capacity of unmelted 5S RNA (whether native or not) evidently exhibits a stronger temperature dependence than does melted 5S RNA. A similar effect has been observed for proteins (Jackson & Brandts, 1970) and for transfer RNAs (Privalov et al., 1975).

Four Salt Conditions: (*A*) *No Added Na^+ or Mg^{2+}*. In the absence of added cations, 5S RNA melts in four stages at relatively low temperature (26 °C < T_m < 42 °C). The total enthalpy of melting (ΔH_{exp}) is small (ca. 285 kcal/mol) as is the thermodynamic stability (ΔG^{298} = 10.4 kcal/mol). In the absence of counterions for the RNA phosphates, intrachain Coulomb repulsions are evidently able to overcome base stacking and base-pair hydrogen bonding with the help of only a little additional heat energy. Tertiary structure may be absent altogether.

(*B*) *In 100 mM NaCl with No Added Mg^{2+}*. Following neutralization of the backbone phosphates by 100 mM Na^+, the melting process broadens to a wider (and higher) temperature range (43 °C < T_m < 62 °C) and resolves into four stages. ΔH_{exp} increases markedly to 371 kcal/mol, as does the thermodynamic stability (ΔG^{298} = 31.5 kcal/mol). The maximum of the composite DSC peak occurs at about 52 °C, in good agreement with T_m = 54 °C obtained from ultraviolet hyperchromism and T_m = 55 °C from FT-IR (Li et al., 1984a). The agreement is important because it shows that the temperature-induced changes in the optical spectrum (which are due primarily to unstacking of bases) account for most of the energy of unfolding seen by DSC in the absence of Mg^{2+}. Therefore, if most of the ΔG^{298} observed by DSC is due to base stacking (as opposed to interactions between base-paired segments, for example), then DSC should provide a good basis for assessing various secondary structural models whose calculated stabilities are based in turn upon optical melting studies of mixtures of complementary homopolymers (see below).

(*C*) *In 10 mM $MgCl_2$ with No Added Na^+*. As previously observed for tRNA (Privalov & Filimonov, 1975), the addition of Mg^{2+} stabilizes the 5S RNA: melting occurs much more cooperatively and at significantly higher temperature (ca. 70 °C). In addition to neutralizing the phosphates, Mg^{2+} evidently acts to link single-stranded segments together, forcing the molecule to hold together until essentially all of the segments have melted. ΔH_{exp} reaches its largest value (480 kcal/mol), as does the thermodynamic stability (ΔG^{298} = 61 kcal/mol).

(*D*) *In 100 mM NaCl and 10 mM $MgCl_2$*. This data set shows that addition of Na^+ actually reduces the total enthalpy of melting produced by Mg^{2+} alone: ΔH_{exp} = 398 kcal/mol and ΔG^{298} = 51 kcal/mol. Again, a similar effect is seen for tRNAs (Privalov & Filimonov, 1978). In particular, it is interesting to note that ΔH and ΔG^{298} for component transitions 1, 2, and 4 are relatively unaffected by Na^+: the principal effect of Na^+ is to destabilize component 3. The DSC composite peak maximum falls at about 72 °C, somewhat higher than T_m = 69 °C from UV hyperchromism and T_m = 57–65 °C from FT-IR (Li et al., 1984a).

One might at first suppose that the additional enthalpy and higher T_m produced by addition of $MgCl_2$ to the 5S RNA are due to increased stability of the macromolecular conformation due to strong attachment of Mg^{2+} to the backbone phosphates. However, because Mg^{2+} at high temperature produces irreversible cleavage of the polyribonucleotide chain (see Results), it is likely that at least part of the Mg^{2+} contribution to ΔH_{exp} is due to breakage of phosphodiester bonds. Thus, the results for 0.1 M NaCl without added $MgCl_2$ probably give the best measure of secondary and tertiary conformational enthalpy for wheat germ 5S RNA.

Number of Base Pairs. In this work, the enthalpies of melting for A·U (9.6 kcal/mol of base pairs), G·C (13.6 kcal/mol), and G·U (7.2 kcal/mol) base pairs are taken from Schott et al. (1981). Their ΔH for A·U melting is in turn based on optical (Neumann & Ackermann, 1969) and calorimetric (Filimonov & Privalov, 1978) experiments on poly(rA)·poly(rU). ΔH for G·C and G·U melting cannot be determined directly: poly(rG)·poly(rfC) does not completely dissociate even at >100 °C (Ornstein & Fresco, 1983), and poly(rG) and poly(rU) do not spontaneously form a duplex polymer in the first place. In these cases, ΔH is estimated from indirect methods (Gralla & Crothers, 1973) based on data from complementary polyribonucleotide sequences containing known relative numbers of A·U, G·C, and G·U pairs.

The number of A·U, G·C, and G·U base pairs for wheat germ 5S RNA under salt condition B (100 mM NaCl, no Mg^{2+}), has been determined by FT-IR (Li et al., 1984a), from which an enthalpy of melting is readily computed:

$$14\text{A·U} + 17\text{G·C} + 5\text{G·U} = 36 \text{ total base pairs}$$

$$(14 \times 9.6 = 134.4) + (17 \times 13.6 = 231.2) + (5 \times 7.2 = 36) = 401.6 \text{ kcal/mol}$$

The DSC value for ΔH_{exp} (see Table I) under these conditions is 371 kcal/mol. The consistency between the DSC and FT-IR values greatly strengthens the credibility of the FT-IR tech-

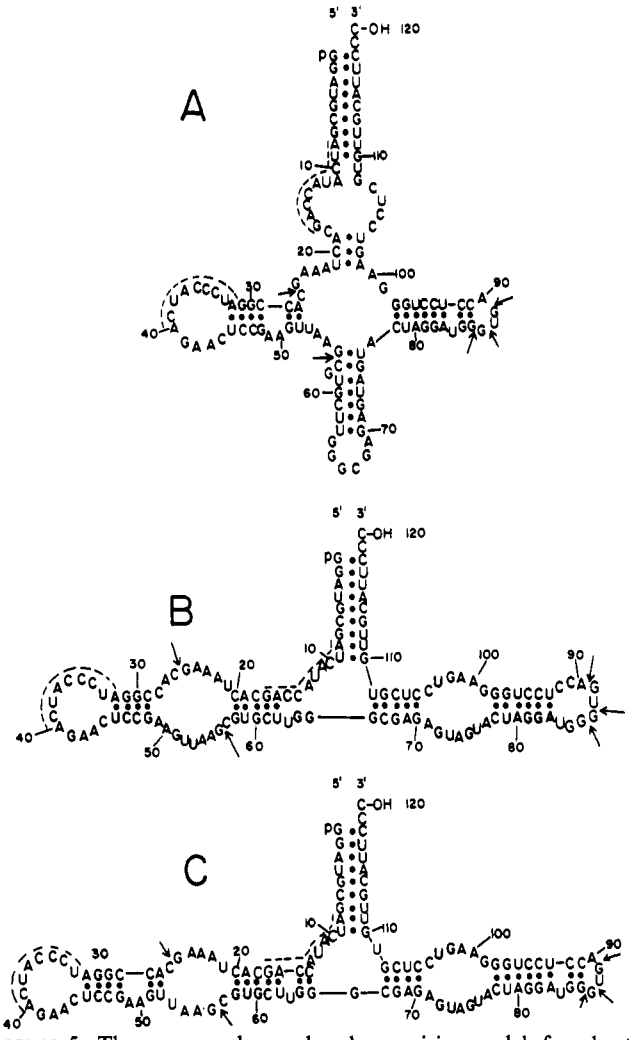

FIGURE 5: Three proposed secondary base-pairing models for wheat germ 5S RNA. For each model, the calculated base-pair enthalpies and free energies of the molecule as a whole are listed in Table IV. (A) Cloverleaf model (Luoma & Marshall, 1978a,b); (B) revised Fox and Woese model; (C) Studnicka et al./Nishikawa and Takemura model.

nique for determination of base pairing in RNA. Since the FT-IR method assumes that all stacked bases are paired (Burkey et al., 1983), both secondary and tertiary base pairs are included in the FT-IR base-pair numbers. However, tertiary base pairs exhibit only about half the enthalpy of melting of secondary base pairs (Privalov & Filimonov, 1978). Thus, the difference in melting enthalpy between the DSC and FT-IR provides a crude estimate of $[(401.6 - 371)/[(9.6 + 13.6)/2)]] \times 2 = 6$ tertiary base pairs in wheat germ 5S RNA.

The proton NMR spectrum of wheat germ 5S RNA is highly resolved throughout the melting range (S.-J. Li and A. G. Marshall, unpublished results), suggesting that the molecule possesses high conformational homogeneity. Thus, it is likely that each DSC scan represents a series of transitions for similar molecules, rather than a sum of transitions from a mixture of initially different conformers.

Secondary Base-Pairing Models. Figure 5 shows three representative secondary base-pairing models for wheat germ 5S RNA. It is tempting, but not necessarily correct, to identify a particular DSC peak with the melting of a particular base-paired segment of the secondary structure. For example, a single DSC peak might well involve the cooperative unfolding of portions of two or more base-paired segments in the secondary/tertiary structure. The present analysis will thus be limited to comparing *total* experimental free energy of melting with that predicted from each of the three models.

Table IV: Total Enthalpy and Free Energy of Melting for Wheat Germ 5S RNA

	ΔH (kcal/mol)	ΔG (kcal/mol)
cloverleaf (Luoma & Marshall, 1978a,b)	360.0	−23.3
Fox & Woese (1975)	326.4	−29.5
Studnicka/Nishikawa	396.8	−32.3
experimental (Table I, condition B)	371.0	−31.5

The total experimental free energy of melting of wheat germ 5S RNA is listed in Table I for all four salt conditions. Rules have been proposed (Tinoco et al., 1973; Salser, 1977) for estimating the free energy and enthalpy of an RNA duplex of known sequence compared to its corresponding single strands at 25 °C in neutral buffer at an ionic strength corresponding most closely to salt condition B. Application of those rules to the proposed secondary structures of Figure 5 leads to the values listed in Table IV.

The experimental total enthalpy of melting from DSC (Table IV) matches most closely to the cloverleaf model (Luoma & Marshall, 1978a,b). The DSC free energy of melting most closely matches the Fox and Woese model, because a Studnicka/Nishikawa model would lead to more secondary base pairs than are detected via DSC. It will be advisable to consider DSC data from several primary sequences before attempting further interpretation of the DSC results. Meanwhile, homonuclear proton nuclear Overhauser experiments now in progress in our laboratory make it possible to identify particular base pairs, whose melting profiles may then be correlated to the DSC results to provide an absolute determination of the secondary structure.

ACKNOWLEDGMENTS

We thank International Multifoods for their gift of wheat germ. We also thank Lee-Hong Chang for helpful discussions.

Registry No. Na, 7440-23-5; Mg, 7439-95-4.

REFERENCES

Barber, C., & Nichols, J. L. (1978) *Can. J. Biochem. 56*, 357–364.

Burkey, K. O., Alben, J. O., & Marshall, A. G. (1983) *Biochemistry 22*, 4223–4226.

Burns, P. D., Luoma, G. A., & Marshall, A. G. (1980) *Biochem. Biophys. Res. Commun. 96*, 805–811.

Chang, L.-H., Burkey, K. O., Alben, J. O., & Marshall, A. G. (1984a) *Biochemistry 23*, 3659–3662.

Chang, L.-H., Li. S.-J., Ricca, T. L., & Marshall, A. G. (1984b) *Anal. Chem. 56*, 1502–1507.

Dawson, R. M. C., Elliott, D. C., Elliott, W. J., & Jones, K. M. (1969) in *Data for Biochemical Research*, 2nd ed., pp 169–179. Oxford University Press, Oxford.

Erdmann, V. A., Wolters, J., Huysmans, E., Vandenberghe, A., & De Wachter, D. (1984) *Nucleic Acids Res. 12*, r133–r166.

Filimonov, V. V., & Privalov, P. L. (1978) *J. Mol. Biol. 122*, 465–470.

Filimonov, V. V., Poetkhin, S. S., Matveev, S. V., & Privalov, P. L. (1982) *Mol. Biol. 16*, 435–444.

Fox, G. E., & Woese, C. R. (1975) *Nature (London) 256*, 505–507.

Freire, E., & Biltonen, R. L. (1978) *Biopolymers 17*, 463–479.

Gralla, J., & Crothers, D. M. (1973) *J. Mol. Biol. 73*, 497.

Jackson, W. M., & Brandts, J. F. (1970) *Biochemistry 9*, 2294–2301.

Kime, M. J., & Moore, P. B. (1983a) *Biochemistry 22*, 2622–2629.
Kime, M. J., & Moore, P. B. (1983b) *Biochemistry 22*, 2615–2622.
Krishnan, K. S., & Brandts, J. F. (1978) *Methods Enzymol. 49*, 3–14.
Li, S.-J., Burkey, K. O., Louma, L., Alben, J. O., & Marshall, A. G. (1984a) *Biochemistry 23*, 3652–3658.
Li, S.-J., Chang, L.-H., Chen, S.-M., & Marshall, A. G. (1984b) *Anal. Biochem. 138*, 465–471.
Luoma, G. A., & Marshall, A. G. (1978a) *Proc. Natl. Acad. Sci. U.S.A. 75*, 4901–4905.
Luoma, G. A., & Marshall, A. G. (1978b) *J. Mol. Biol. 125*, 95–105.
Luoma, G. A., Burns, P. D., Bruce, R. E., & Marshall, A. G. (1980) *Biochemistry 19*, 5456–5462.
MacKay, R. M., Spencer, D. F., Doolittle, W. F., Gray, M. W. (1980) *Eur. J. Biochem. 112*, 561–576.
Marshall, A. G., & Smith, J. L. (1980) *Biochemistry 19*, 5955–5959.
Matveev, S. V., Filimonov, V. V., & Privalov, P. L. (1982) *Mol. Biol. 16*, 990–999.
Morikawa, K., Kawakami, M., & Takemure, S. (1982) *FEBS Lett. 145*, 194–196.
Neumann, E., & Ackermann, Th. (1969) *J. Phys. Chem. 73*, 2170.
Nishikawa, K., & Takemura, S. (1974) *FEBS Lett. 40*, 106–109.
Ohta, S., Maruyama, S., Nitta, K., & Sugai, S. (1983) *Nucleic Acids Res. 11*, 3363–3373.
Ornstein, R. L., & Fresco, J. R. (1983) *Biopolymers 22*, 2001–2016.
Privalov, P. L. (1974) *FEBS Lett. 40*, S140–S153.
Privalov, P. L., & Filimonov, V. V. (1978) *J. Mol. Biol. 122*, 447–464.
Privalov, P. L., Filimonov, V. V., Venkstern, T. V., & Bayev, A. A. (1975) *J. Mol. Biol. 97*, 279–288.
Salemink, P. J. M., Raue, H. A., Heerschap, A., Planta, R. J., & Hilbers, C. W. (1981) *Biochemistry 20*, 265–272.
Salser, W. (1977) *Cold Spring Harbor Symp. Quant. Biol. 42*, 985–1002.
Schott, F. J., Grubert, M., Wangler, W., & Ackermann, T. (1981) *Biophys. Chem. 14*, 25–30.
Studnicka, G. M., Eiserling, F. A., & Lake, J. A. (1981) *Nucleic Acids Res. 9*, 1885–1904.
Tinoco, I., Jr., Borer, P. N., Dengler, B., Levine, M. D., Uhlenbeck, O. C., Crothers, D. M. & Gralla, J. (1973) *Nature (London) New Biol. 246*, 40–41.

Evolutionary Aspects of Accuracy of Phenylalanyl-tRNA Synthetase. Accuracy of the Cytoplasmic and Chloroplastic Enzymes of a Higher Plant (*Phaseolus vulgaris*)†

Reinhard Rauhut, Hans-Joachim Gabius, and Friedrich Cramer*
Max-Planck-Institut für Experimentelle Medizin, Abteilung Chemie, D-3400 Göttingen, Federal Republic of Germany
Received November 15, 1984

ABSTRACT: The phenylalanyl-tRNA synthetases from cytoplasm and chloroplasts of bean (*Phaseolus vulgaris*) leaves employ different strategies with respect to accuracy. The chloroplastic enzyme that is coded for by the nuclear genome follows the pathway of posttransfer proofreading, also characteristic for enzymes from eubacteria and cytoplasm and mitochondria of lower eukaryotic organisms. In contrast, the cytoplasmic enzyme uses pretransfer proofreading in the case of noncognate natural amino acids, characteristic for higher eukaryotic organisms and archaebacteria. Dependent on the nature of the noncognate amino acid, pretransfer proofreading in this case occurs without tRNA stimulation or with tRNA stimulated with no or little effect of the nonaccepting 3′-OH group of the terminal adenosine. The fundamental mechanistic difference in proofreading between the heterotopic intracellular isoenzymes of the plant cell supports the idea of the origin of the chloroplastic gene by gene transfer from a eubacterial endosymbiont to the nucleus. Origin by duplication of the nuclear gene, as indicated for mitochondrial phenylalanyl-tRNA synthetases [Gabius, H.-J., Engelhardt, R., Schroeder, F. R., & Cramer, F. (1983) *Biochemistry 22*, 5306–5315], appears unlikely. Further analyses of the ATP/PP_i pyrophosphate exchange and aminoacylation of $tRNA^{Phe}$-C-C-A(3′NH_2), using 11 phenylalanine analogues, reveal intraspecies and interspecies variability of the architecture of the amino acid binding part within the active site.

It is well established that the correct aminoacylation of the cognate tRNA with the proper amino acid by aminoacyl-tRNA synthetases strongly contributes to the overall fidelity of protein synthesis (Cramer et al., 1979; Yarus, 1979). Recently we have presented evidence in the case of the phenylalanyl-tRNA synthetases that the strategies to achieve the high level of fidelity in this process differ among various organisms at different branches of the evolutionary tree (Gabius et al., 1983a,b). Between the various organisms the contribution of primary recognition of the amino acid and the successive corrective step, proofreading, to fidelity differs markedly. Within the eukaryotes even the proofreading mechanism, whereby misactivated intermediates are hydro-

† Dedicated to Prof. Dr. W. Lamprecht on the occasion of his 60th birthday.

0006-2960/85/0424-4052$01.50/0